Available online at www.sciencedirect.com

ScienceDirect

Procedia Manufacturing 00 (2019) 000–000

Procedia MANUFACTURING

www.elsevier.com/locate/procedia

23rd International Conference on Material Forming (ESAFORM 2020)

Influence of the Choice of the Parameters on Constitutive Models and their Effects on the Results of Ti6Al4V Orthogonal Cutting Simulation

Nithyaraaj KUGALUR-PALANISAMY[a,*], Edouard RIVIÈRE-LORPHÈVRE[a], François DUCOBU[a] and Pedro-José ARRAZOLA[b]

[a]*University of Mons, Faculty of Engineering, Machine Design and Production Engineering Lab - Belgium*
[b]*Mondragon University, Faculty of Engineering, Mechanical and Manufacturing Department - Spain*

* Corresponding author. Tel.: +32 653 740 92; *E-mail address:* nithyaraaj.kugalurpalanisamy@umons.ac.be

Abstract

A pertinent set of parameters is equally important as a constitutive model that describes the material behavior in modeling and finite element simulation of the machining process. The purpose of this study is to show the influence of the parameters on constitutive models by comparing and investigating three constitutive laws. The first is the original Johnson-Cook model, the second is the modified Johnson-Cook model that takes the strain softening behavior into account and the third is the modified Johnson-Cook model that introduces a temperature dependent hardening factor. This paper deals with the modelling and simulation of the orthogonal cutting process with those three constitutive models with different sets of constitutive model parameters and highlights their influence on the results. Forces and chip morphology from the numerical simulations are compared with an experimental orthogonal cutting reference for validation and determination of the best combination.

*Keywords:*Orthogonal Cutting Simulation; FEA;Constitutive models;Influence of Parameters.

1. Introduction

The numerical modelling of machining by the process of chip removal with a cutting tool takes into account complex phenomena which involves large strains, strain rates and very high temperature. The Finite element modelling is widely employed by the researchers to model the simplified orthogonal cutting configuration [1].

A reliable constitutive model is always a prime factor in developing a finite element model [1]. Therefore, a well-defined flow stress model that considers the strain, the strain rate, the temperature, the hardening, the viscosity and the loading history of the material is inevitable in numerical modelling of metal cutting process. An accurate material constitutive model that describes the behavior of the material during the orthogonal cutting process remains a challenge and is a key factor influencing the prediction accuracy in cutting process. Many material constitutive models have been developed in the past years. Because of their simplicity, empirical models are widely considered. Among those, the Johnson-Cook (JC) model [2] is highly employed in modelling and simulation studies. Indeed, numerous sets of parameters are found in literature and this variation is due to different thermal treatments, experimental conditions, chemical compositions of the material.

This paper highlights the importance and influence of the choice of the parameters by comparing and analyzing finite element simulation of Johnson-Cook model [2] with the modified Johnson-Cook model from Calamaz et al. [3] that takes the strains softening behavior into account and the Modified Johnson-Cook from Hou et al. [4] that takes into account temperature dependent hardening factor and its coupled effects between strain and temperature. Along with sets of parameters acquired from the reference's Seo et al. [5], Calamaz et al. [3] and Hou et al. [4]. Each constitutive law is

treated with three different sets of parameters making a total of nine models. The results from the nine simulations are analyzed, the forces and chip morphologies are compared, and they are validated with an experimental reference.

2. Material Constitutive Models

The empirical or phenomenological model describes the high strain rate and high temperature flow stress response of metals in machining. These models consider the variables of deformations such as the plastic strain ε, plastic strain rate $\dot{\varepsilon}$, and temperature T under macroscopic scale.

2.1 Johnson–Cook Constitutive Model

The most widely used thermo-mechanical model that links plastic, viscous and thermal aspects observed during orthogonal machining process is the robust Johnson-Cook model [2]. Its flow stress is expressed by the following Eq. (1):

$$\sigma = [A + B\,\varepsilon^{n}]\left[1 + C ln\frac{\dot{\varepsilon}}{\dot{\varepsilon}_0}\right]\left[1 - \left(\frac{T - T_{room}}{T_{melt} - T_{room}}\right)^{m}\right] \quad (1)$$

Where A, B, C, n, m are the constants that depend on the material and are determined by material tests. A is the yield strength, B the hardening modulus, n the strain-hardening exponent, C the strain rate sensitivity and m is the thermal sensitivity. Constants B and n reports the strain hardening. T_{melt} and T_{room} are the melting temperature and the room temperature respectively, while $\dot{\varepsilon_0}$ is the reference strain rate.

The JC model is meaningful in certain operating ranges of strains and strain-rates (strains up to 0.5 and strain rates lower than 10^4 s^{-1}) [1] but fails to capture high strain material behavior in machining, where the flow stresses are difficult to measure by existing material testing devices [2]. Thermal softening is defined as the flow stress drops with the increased temperature regardless of plastic strain. In addition, JC model does not account for softening observed at the strains and temperatures in the primary shear zone, which is characteristic of metals that exhibit shear banding. This leads to a modified or updated version of Johnson-Cook model.

2.2 *Modified Johnson–Cook model by CALAMAZ*

In order to overcome their drawbacks, numerous models are proposed for Ti6Al4V alloy to describe the dynamic deformation behavior during cutting process. A Modified version have been suggested by Calamaz et al. [3] to include novel multiplicative strain and temperature dependent. In order to model strain softening effect at the high-speed machining process, Calamaz et al. [3] introduced a TANH (hyperbolic tangent) term into the Johnson-Cook flow stress model. The material flow stress for TANH model is expressed by the following Eq. (2):

$$\sigma = \left[A + B\,\varepsilon^{n}\left(\frac{1}{exp(\varepsilon^{a})}\right)\right]\left[1 + C ln\frac{\dot{\varepsilon}}{\dot{\varepsilon}_0}\right]\left[1 - \left(\frac{T - T_{room}}{T_{melt} - T_{room}}\right)^{m}\right]$$

$$\left[D + (1 - D)\,tanh\left(\frac{1}{(\varepsilon + S)^{c}}\right)\right] \quad (2)$$

Where,

$$D = \left[1 - \left(\frac{T}{T_{melt}}\right)^{d}\right] \quad \text{and} \quad S = \left[1 - \left(\frac{T}{T_{melt}}\right)^{b}\right]$$

Parameters A, B, C, n, m have the same meaning of JC model and the new constants a, b, c and d are introduced by TANH law.

In the above equation, the first term, strain hardening function is modified by including flow softening at higher strain values, the second term on strain rate and the third term on thermal softening function remains unaltered and a fourth term on temperature-dependent flow softening condition were added.

2.3 Modified Johnson–Cook model by HOU

Hou et al [4] introduced a temperature function into the work hardening term to describe the phenomenon of temperature dependent hardening effect for better prediction of flow stress behavior of Ti6Al4V alloy under loading condition of high strain rate and temperature.

A modified JC model was proposed (Eq. 3) by coupling logarithmic strain hardening rate and thermal sensitivity coefficient along with the strain function.

It was concluded that strain hardening rate Q of Ti6Al4V alloy has no noticeable strain rate sensitivity but an obvious temperature sensitivity. The strain or work hardening rate Q is a function of temperature. The flow stress equation expressed by the following Eq. (3)

$$\sigma = \left[A + B\left(1 + m_1 \ln\frac{T}{T_{room}}\right)\varepsilon^{n}\right]\left[1 + C ln\frac{\dot{\varepsilon}}{\dot{\varepsilon}_0}\right]\left[1 - \left(\frac{T - T_{room}}{T_{melt} - T_{room}}\right)^{m}\right] \quad (3)$$

Where, m_1 is the thermal sensitivity coefficient with the increasing strain, and the rest of all parameters have the same meaning as JC model.

3. Constitutive Models Parameters for Modelling of Machining Process of Ti6Al4V

Besides the implementation of the constitutive models in numerical modelling software's, the large availability of parameter sets for the same material in the literature initiate the discussion. Indeed, Ducobu et al. [6] extensively analyzed 20 different sets of Johnson-Cook parameters from the literature for Ti6Al4V by comparing the outputs of a Coupled Eulerian-Lagrangian orthogonal cutting model with the experimental results and concluded that the parametric set from SEO et al. [5] gives near accurate results for the forces and chip thickness.

From the above discussion the set of parameters for JC model is adopted from Seo et al. [5], the set of parameters for JC-Calamaz is adopted from the work of Calamaz et al. [2] and set of parameters for JC-Hou is acquire from Hou et al. [3]. The sets of parameters are mentioned as 1, 2 and 3 correspondingly throughout the article.

The sets of parameters adopted for three models are reported in Table 1.

Table 1. Sets of parameters considered for this study - 1 [5], 2 [2] and 3 [3].

1		2		3	
A (MPa)	997.9	A (MPa)	968	A (MPa)	920
B (MPa)	653.1	B (MPa)	380	B (MPa)	400
C	0.0198	C	0.02	C	0.042
m	0.7	m	0.577	m	0.633
n	0.45	n	0.421	n	0.578
T_{room}(K)	298	T_{room}(K)	298	T_{room}(K)	293
T_{melt}(K)	1878	T_{melt}(K)	1878	T_{melt}(K)	1933
		a	1.6	m_1	0.158
		b	0.4		
		c	6		
		d	1		

To highlight the influence of parameters on numerical modelling of cutting process simulation the three different sets of parameters are considered with the three constitutive models making a total of nine simulations (3 constitutive laws * 3 sets of parameters).

The stress vs strain curve evolution for the JC with set 1 parameters, JC-Calamaz with set 2 parameters and JC-Hou with set 3 parameters at fixed temperatures of T=573 K and T=973 K for strain rate of $\dot{\varepsilon} = 10000\ s^{-1}$ is plotted in Fig 1 and Fig 2 respectively.

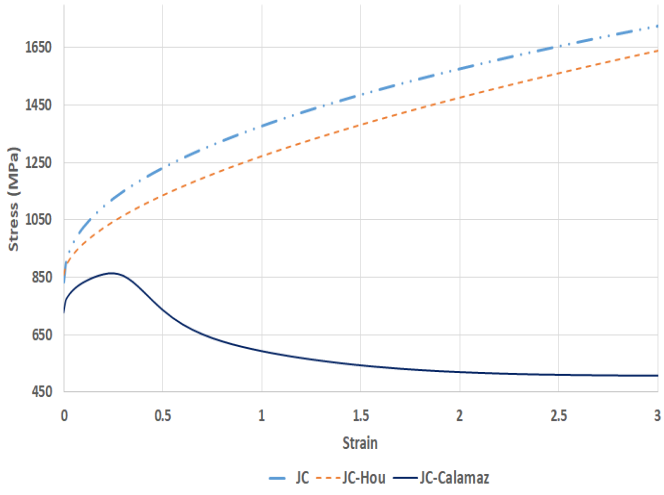

Fig. 1. Stress-strain curves of JC, JC-Calamaz and JC-Hou at T=573 K and $\dot{\varepsilon_0}$ = 10 000 s^{-1}

From the evolution of stress-strain curves in Fig.1 and Fig.2 we can see that JC-Calamaz law takes the softening behavior into account and the JC-Hou law that consider the temperature dependent hardening effect shows a significant difference in the evolution of stress with respect to strain at higher temperature and strain rate when compared.

Indeed, it is indispensable to note that the initial stress value of JC-Calamaz is low when compared with initial stress value of other two constitutive models considered in this study and this might influence the result to great extent.

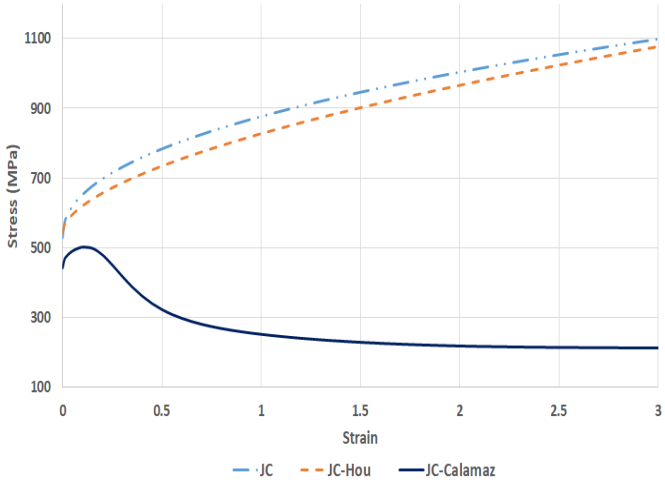

Fig. 2. Stress-strain curves of JC, JC-Calamaz and JC-Hou at T=973 K and $\dot{\varepsilon_0}$ = 10 000 s^{-1}

Fig.3. shows flow stress evolution curves for the three constitutive models with three sets of paraments respectively. When compared, the stress-strain evolution with set 2 parameters shows a low initial stress value regardless of the constitutive laws, where the other sets of parameters show approximately same initial stress value, however differences in their evolution are clearly noted.

The stress evolution curves confirm the influence of the choice of the sets of parameters for each constitutive model and their capability in influencing the results.

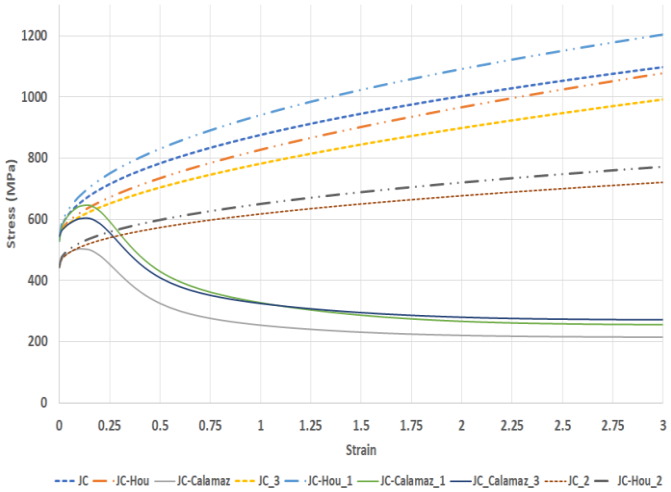

Fig. 3. Stress-strain curves of three constitutive law with three sets of parameters at T=973 K and $\dot{\varepsilon_0}$ = 10 000 s^{-1}

4. Finite Element Model

A two-dimensional (2D) plane strain model with coupled thermo-mechanical analysis using orthogonal cutting assumption was considered for the study. An explicit Lagrangian finite element formulation is employed to simulate orthogonal cutting process of Ti6Al4V alloy by a commercial FEA solver ABAQUS.

In this FE model, the tool moves over the workpiece as the workpiece is fixed. The work piece is modeled as a rectangular

block of 1 mm x 1 mm and is meshed with element size of 5 µm×5 µm [10] square linear quadrilateral elements of type CPE4RT. Tungsten carbide is selected as a tool material and the linear elastic law is imposed.

The tool geometry is defined by the rake angle of 15°, the clearance angle of 2° and the cutting-edge radius of 20 µm for a cutting condition involving a cutting speed of 30 m/min and the uncut chip thickness of 60 µm. The basic geometry and the boundary conditions are illustrated in Fig. 4. A simple Coulomb's friction law is employed to model friction between the tool-chip interface with a friction coefficient of 0.2 [8]. The thermal properties are adopted from the reference [8]. The initial temperature for tool and workpiece is set according to the parameter chosen for the simulation from Table 1.

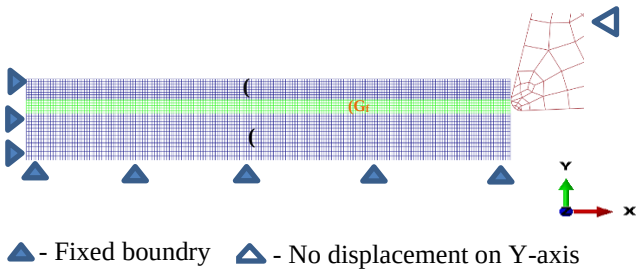

Fig. 4. Finite element model with Initial geometry, initial mesh structure, boundary conditions and fracture energy in region 1 and 2

4.1 Damage Modelling

The chip separation criteria in other words damage or fracture initiation and damage evolution models are of equal importance in defining numerical models for orthogonal cutting simulation using Lagrangian formulation. For chip separation/chip formation, Johnson-Cook damage model [9] is considered.

$$D = \Sigma \frac{\Delta\varepsilon}{\varepsilon_f} \tag{4}$$

Where $\Delta\varepsilon$ is the plastic strain increment ε_f is the effective plastic strain to fracture and D is an internal (state) variable that increases monotonically with plastic deformation up to a value of 1, when damage initiation occurs. The term ε_f, takes the form

$$\varepsilon_f = \left[d_1 + d_2 \exp d_3 \left(\frac{-p}{\bar{\sigma}}\right)\right]\left[1 + d_4 ln\left(\frac{\dot{\varepsilon}}{\dot{\varepsilon}_0}\right)\right]\left[1 + d_5\left(\frac{T - T_{room}}{T_{melt} - T_{room}}\right)\right] \tag{5}$$

The JC failure model parameters adopted for Ti6Al4V are reported in Table 2.

Table 2. Johnson–Cook failure parameters [10].

Material	d_1	d_2	d_3	d_4	d_5
Ti6Al4V	-0.09	0.27	0.48	0.14	3.87

The methodology of fracture mechanics was acquired for this model leads to the usage of two different values of fracture energy as an input data in Abaqus/Explicit, where fracture energy in region-I $(G_f)_I$ is defined by tensile mode (mode I: opening mode) and fracture energy region-II $(G_f)_{II}$ is defined by shearing one (mode II: sliding mode acting parallel to the plane of the fracture) [9]. The region-I is the layer of chip and region-II is the layer where the tool passes during cutting process [10]. The thickness of the regions is given by:

- Thickness of the region I = uncut chip thickness – cutting edge radius of the tool
- Thickness of the region II = cutting edge radius + one element

The fracture energy is given by equation 7 [11]:

$$\left(G_f\right)_{I,II} = \left(\frac{1-\nu^2}{E}\right)\left(K_c^2\right)_{I,II} \tag{6}$$

Where K_c is fracture toughness, E is the Young's modulus and ν is Poisson's ratio.

A predictive model is developed for the above cutting conditions and methodologies, only the constitutive equations are changed for the study. With this predictive model a total of nine finite element simulations were carried out by considering three sets of parameters with each constitutive model.

5. Numerical results, Comparisons and Discussions.

5.1 Experimental Reference

The Experimental reference is considered from the work performed by Ducobu et al. [7] on orthogonal cutting of Ti6Al4V on a high-speed milling machine shown in Fig. 5 with the same cutting condition as the model for uncut chip thickness of 60 µm. The cutting force value, feed force value and chip morphology acquired from the experimental reference are compared with the numerical results.

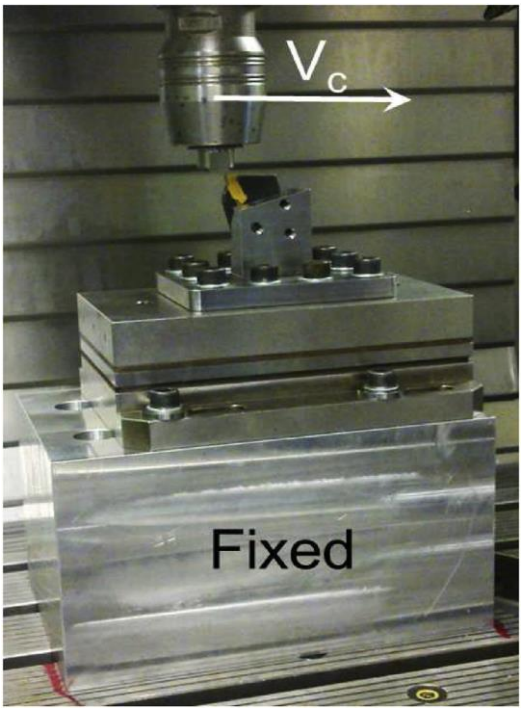

Fig. 5. Cutting configuration on the milling machine [7].

A continuous chip was observed from the orthogonal cutting experiment for this cutting condition. The chip observed from the experiment is shown in Fig 6. The RMS values of cutting force (F_C) was 111 ± 2 N/mm, the feed force (F_f) was 44 ± 1 N/mm and the and chip thickness ($h^{'}$) was 0.080 ±0.04 mm.

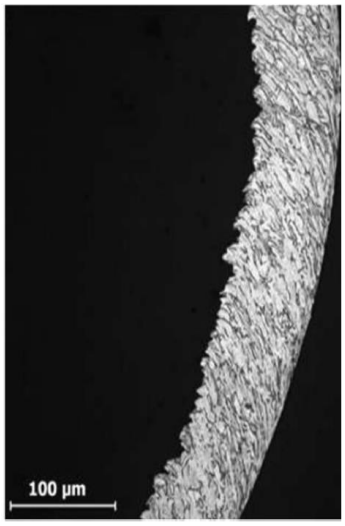

Fig. 6. Experimental reference Chip morphology for uncut chip thickness of 60 µm [7].

5.2 Numerical Results

Initially the temperature differences in the deformation zones and the chip morphologies are compared and analyzed for the three constitutive equations with the native set of parameters (i.e. JC with set 1 parameters, JC-Calamaz with set 2 parameters and JC-Hou with set 3 parameters. The temperature of the numerically computed chip for JC, JC-Hou, and JC-Calamaz is analyzed at 1200 µs. The temperature is maximum in the secondary deformation zone as expected.

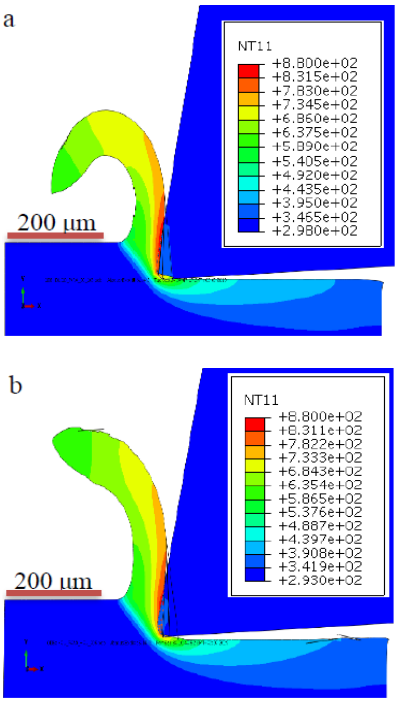

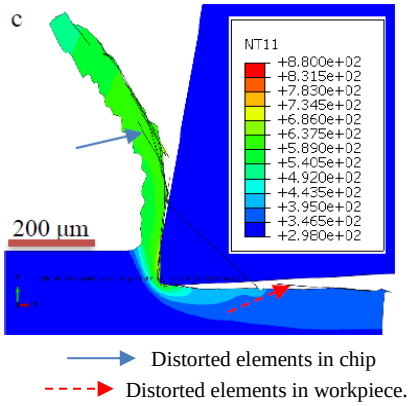

Fig. 7. Temperature contours (in K) of the numerical chip at 1200 µs (a) JC; (b) JC-Hou; (c) JC-Calamaz.

The temperatures for JC-Hou is higher than JC and JC-Calamaz, it's worth noting that the temperature in the secondary deformation zone for JC-Calamaz is very less when compared with JC and JC-Hou and that can be explained by the level of stresses. In addition, deformed and elongated elements are observed in JC-Calamaz and are highlighted in Fig 6(c).

The chips morphologies are compared for the three different constitutive models. The numerical chips of JC and JC-Hou are continuous, as expected but the numerical chip of JC-Calamaz is not continuous (slightly serrated chip) contrary to the experimental reference for this particular condition. This can be explained by the fact that JC-Calamaz model and its parameters are optimized for cutting conditions considered by Calamaz et al. [3]

The RMS forces values are calculated and compared in Table 2. The RMS values of cutting force and feed force for JC-Hou is exactly same as experimental reference when compared with JC model. But the force values of JC-Calamaz are far behind the experimental values.

Furthermore, to confirm the influence of the choice of the parameters on constitutive models, only the sets of parameters are interchanged in the constitutive laws (i.e. JC with set 3 parameters (JC_3), JC with set 2 parameters (JC_2) and JC-Hou with set 1 parameters (JC-Hou_1), JC-Hou with set 2 parameters (JC-Hou_2), JC-Calamaz with set 1 parameters (JC-Calamaz_1) and JC-Calamaz with set 3 parameters (JC-Calamaz_3)) of the predictive FEA model.

The numerical chips of JC model are compared to JC_3 and JC_2 from Fig.8. All the chips are continuous, however differences in the chip thickness are noted especially the chip is thinner for the JC_2 model.

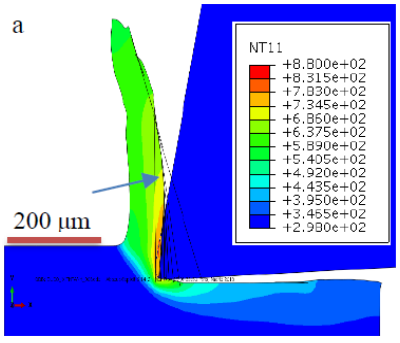

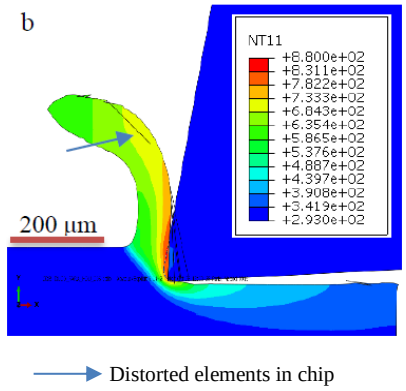

Fig. 8. Temperature contours (in K) of the numerical chip at 1200 µs (a) JC_ 2; (c) JC_3.

In addition, highly distorted and elongated elements are observed with the JC_2 model which implies the influence of the set of parameters. On comparison of above three models the feed force RMS (Root Mean Square) value of JC_3 is near to the experimental result. The thickness of the chip is reduced when the feed force is higher as the feed force is inversely linked with chip thickness in accordance with the references [6,11].

The temperature differences in the secondary shear zone are clearly observed, where the temperature in secondary deformation zone of JC_3 is comparatively high when compared to the JC and JC_2. These temperature differences are analyzed with cutting force RMS values and it is observed that temperature is directly linked with cutting force.

Further comparison is made for the numerical chips of JC-Hou model with JC-Hou_1 and JC-Hou_2 from Fig.9. The chips are continuous with differences in the chip thickness as expected. In addition, highly distorted and more elongated elements are observed with the JC-Hou_2 model.

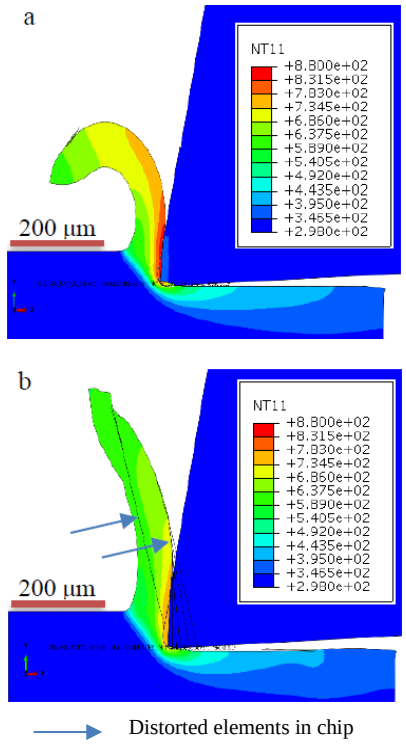

Fig. 9. Temperature contours (in K) of the numerical chip at 1200 µs (a) JC-Hou_1 (b) JC-Hou_2.

The higher feed force RMS value of JC-Hou_2 leads to thinner chip when compared with the HOU, JC-Hou_1 and experimental reference, which implies RMS values of feed force is inversely linked to the thickness of the chip. The RMS cutting force value of JC-Hou model is exactly the same as the experimental reference. Whereas the RMS value of cutting force from other two models are less than the experimental value.

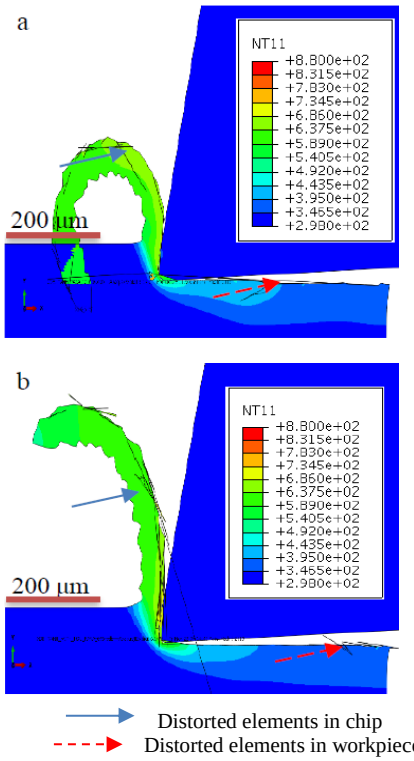

Fig. 10. Temperature contours (in K) of the numerical chip at 1200 µs (a) JC-Calamaz_1 (b) JC-Calamaz_3.

The numerical chips of JC-Calamaz, JC-Calamaz_1, JC-Calamaz_3 from Fig.6(c), Fig.9 are not continuous. Instead they produce slightly serrated chips. Indeed, the temperature differences are seen. In addition, highly distorted and more elongated elements are observed in the chip as well as on the surface of the workpiece. In addition, simulated forces from these three models are highly distinct to values observed from the experiments.

5.3 Discussion

The comparison of nine simulations with the experimental reference shows that the JC and JC-Hou constitutive models with any of the three sets of the parameters produce continuous chip as expected and same as the experimental reference, but the JC_Calamaz model produces serrated chip. The temperature in the secondary deformation zone and the chip morphology of the models JC and JC-Hou models with set 3 parameters are quite consistent, but very distinct from set 2 parameters when compared with the experimental results.

Eventually the feed force, the cutting force RMS values and the chip thickness of JC-Hou model with set 3 parameters are exactly same as experimental value which shows the importance of temperature dependent strain hardening effect on the deformation behavior of Ti6Al4V alloy during machining process.

Table 3. RMS cutting force (F_c), feed force (F_f) and chip thickness (h') summary and Δ_x differences with the experimental forces results

MODELS	Parameters set	Fc (N/mm)	ΔFc (%)	F_f (N/mm)	ΔF_f (%)	h' (mm)	$\Delta_{h'}$ (%)
EXPERIMENTS		113 ± 2	-	44 ± 1	-	0.080 ±0.04	-
	DUCO	106	6	50	5	0.077	-
JC	HOU	108	4	48	3	0.079	-
	CALA	98	14	53	8	0.075	0.001
	DUCO	107	5	42	1	0.087	0.003
HOU	HOU	111	-	46	1	0.081	-
	CALA	99	13	51	6	0.076	-
	DUCO	88	24	54	9	*	-
TANH	HOU	91	21	49	7	*	-
	CALA	82	30	60	15	*	-

The chip type is serrated for TANH model. They are therefore, not considered for comparison with continuous chips

6. Conclusion

In this paper, the influence of the choice of a set of parameters for the JC and modified JC constitutive material (TANH, HOU) models has been studied with three different sets of parameters adopted from the literatures for uncut chip thickness of 60 μm. The results from the nine simulations have been verified by comparing the RMS values of the C cutting force, feed force, chip morphology, chip thickness with the experimental reference.

Significant differences in the values of the parameters of the sets directly influence the stress level values even though the same material is considered. From the experimental reference we expect the chip morphology to be continuous. However, the TANH model with any sets of the parameters produces slightly serrated chip contradiction to the experimental ones for this particular cutting condition. This might be explained by the fact that the formulation and parameters for TANH are identified for different cutting conditions and also concerns the experimental conditions, the thermal treatments and history of the alloy.

From the result and discussion of this study. All the numerical simulations with HOU sets of the parameters show a notable improvement in terms of forces, chip thickness when compared with the other two sets of the parameters.

Overall for this particular cutting condition, the predictive finite element model along modified JC constitutive models of HOU with the parameters identified by HOU et al. [3] is well capable to accurately predict the cutting forces, feed force and chip thickness.

A direct link was observed between the RMS value of the cutting force and the temperature in the secondary shear zone and an inverse link between chip thickness and the RMS value of the feed force.

Acknowledgements

Computational resources have been provided by the Consortium des Équipements de Calcul Intensif (CÉCI), funded by the Fonds de la Recherche Scientifique de Belgique (F.R.S.-FNRS) under Grant No. 2.5020.11.

References

[1] Arrazola PJ, Ozel T, Umbrello D, Davies M, Jawahir IS. Recent advances in modelling of metal machining processes. CIRP Annals - Manufacturing Technology. 2013 Aug 12;62(2):695-718.

[2] Johnson GR, Cook WH. A constitutive model and data for metals subjected to large strains, high strain rates and high temperatures. in: Proceedings of the seventh international symposium on ballistics. The Hague, The Netherlands: 1983. 541–547.

[3] Calamaz M, Coupard D, Girot F. A new material model for 2D numerical simulation of serrated chip formation when machining titanium alloy Ti-6Al-4V. Int J Mach Tools Manuf 2008;48:275–288.

[4] Hou X, Liu Z, Wang B, Lv W, Liang X, Hua Y. Stress-Strain Curves and Modified Material Constitutive Model for Ti-6Al-4V over the Wide Ranges of Strain Rate and Temperature. Materials (Basel) 2018;11(6):938.

[5] Seo S, Min O, Yang H. Constitutive equation for Ti-6Al-4V at high temperatures measured using the SHPB technique. Int J Impact Eng 2005;31:735–754.

[6] Ducobu F, Rivière-Lorphèvre E, Filippi E. On the importance of the choice of the parameters of the Johnson-Cook constitutive model and their influence on the results of a Ti6Al4V orthogonal cutting model. Int J Mech Sci 2017;122:143–155.

[7] Ducobu F, Rivière-Lorphèvre E, Filippi E. Experimental contribution to the study of the Ti6Al4V chip formation in orthogonal cutting on a milling machine. Int J Mater Form 2015;8:455–468.

[8] William D, Callister. Materials Science and Engineering. An Introduction third ed. New York: Wiley; 1994.

[9] Johnson GR, Cook WH. Fracture characteristics of three metals subjected to various strains, strain rates, temperatures and pressures. Eng Fract Mech 1985;21:31-48.

[10] Kay G. Failure Modeling of Titanium-6Al-4V and 2024-T3 Aluminum with the Johnson-Cook Material Model. United States: 2002.
[11] Zhang Y C, Mabrouki T, Nelias D, Gong Y D. Chip formation in orthogonal cutting considering interface limiting shear stress and damage evolution based on fracture energy approach. Finite Elements in Analysis and Design 2011;47:850-863.
[12] Mabrouki T, Girardin F, Asad M. Numerical and experimental study of dry cutting for an aeronautic aluminium alloy (A2024-T351), International Journal of Machine Tools and Manufacture 2008;48:1187-1197.
[13] Kugalur-Palanisamy N, Riviere-Lorphèvre E, Arrazola PJ, Ducobu F. Comparison of Johnson-Cook and modified Johnson-Cook material constitutive models and their influence on finite element modelling of Ti6Al4V orthogonal cutting process. AIP Conference Proceedings 2019; 2113:080009.